Supplementary data

Section 1: equipment stability measurements.

To perform the accurate quantitative analysis of Methylene blue (MB) degradation, the equipment characteristics including excitation stability, wavelength dependent detector sensitivity, detector stability and water sealability should be carefully examined. A Teflon reflector has been to determine the excitation intensity as a function of wavelength. The results are shown in Fig. S1.

By applying a wavelength versus excitation intensity scanning mode, as shown in Fig S1a, the constant excitation intensity (I_0 in Eq(8)) has been observed in the range of 300 nm to 625 nm, suggesting the MB florescence is only relevant with extinction coefficient $\varepsilon(\lambda)$ and MB concentration C in Eq (8) (Theory section). By fixing the excitation at certain wavelength, the continuous excitation intensity as a function of time is obtained (Fig. S1b), in Fig S1b, the recorded excitation remains constant, which indicating a robust excitation and detector stability in our equipment. Finally, the $I_F(t)$ (Eq (12)) from a pure MB solution were recorded from multiple monochromatic excitation, the results are shown in Fig. S1(c-h). As shown from Fig S1(i-j), a constant $I_F(t)$ were found under excitation of 340 nm, 400 nm, 450 nm, 550 nm and 625 nm, which refers the water evaporation induced MB concentration (C_{MB}) increasing is not an issue for our in-situ experiment set up. To conclude, we have proven our equipment for WIDFS set up contains robust excitation and detector stability with perfect water sealability.

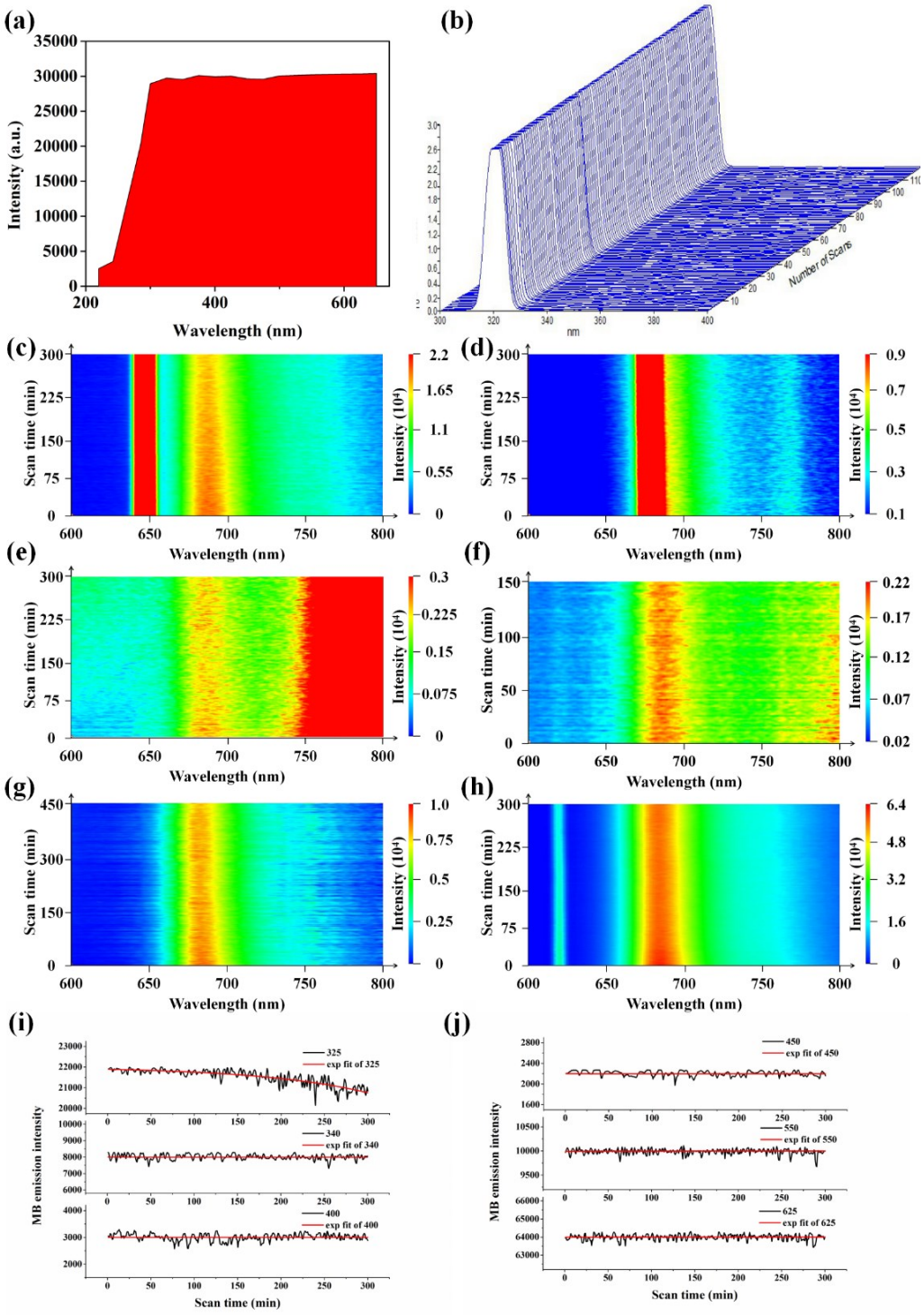

Fig. S1. Equipment stability. a. the wavelength - dependent intensity of the light source, **b.** stabilization of fixed wavelength light source in in-situ measurements; **The MB photodegradation without samples. c**, under 325 nm illumination. **d**, under 340 nm illumination without samples. **e**, under 400 nm illumination. **f**, under 450 nm illumination. **g**, under 550 nm illumination. **h**, under 625 nm illumination. **g**, exp fit of fig S3c,d and e. **h**, exp fit of fig S3f,g and h.

Section 2: Correlation between MB fluorescence intensity and MB concentration

In theory section Eq (8), to investigate the MB degradation rate through fluorescence intensity, the I_F and C_{MB} should be correlated. By measuring the IF for different MB concentration, the results are shown in Fig. S2(a-c). As shown in Fig. S2d, the MB emission intensity and excitation wavelength are strongly correlated. The MB emission intensity increased linearly with the rising concentration of MB solution, which indicates the linear approximation of pollutant concentration and florescence intensity in manuscripts equation (6) is generally valid for our case. Therefore, the pure MB concentration $\boldsymbol{C}_{MB}$ as a function of MB emission intensity $\boldsymbol{I}_{MB}$ can be used as a reference to determine the MB degradation rate. For an example, by extrapolating the emission intensity at 688 nm under 325 nm illumination in Fig. S2a, the established $\boldsymbol{I}_{MB}$~ $\boldsymbol{C}_{MB}$ function is in Fig. S2d (black line). And the experimental data of 340 nm, and 450 nm excitation wavelength were be processed by applying this approach. The results can be found in Fig S2d.

A special case has been observed at 340 nm excitation, where the secondary excitation peak corresponding to excitation wavelength with MB florescence wavelength is merged, which create problem for MB fluorescence peak extrapolation. In order to extract the MB florescence maximum intensity as a function of acquisition time, a Gaussian function convolved with Asymmetry double sigmoidal (Asym2sig)

function is applied to fit the experimental spectrum (Fig. S2(e-f)), by excluding the Gaussian profile from the experimental spectrum, the MB florescence intensity under 340 nm excitation can be then reasonable confirmed.

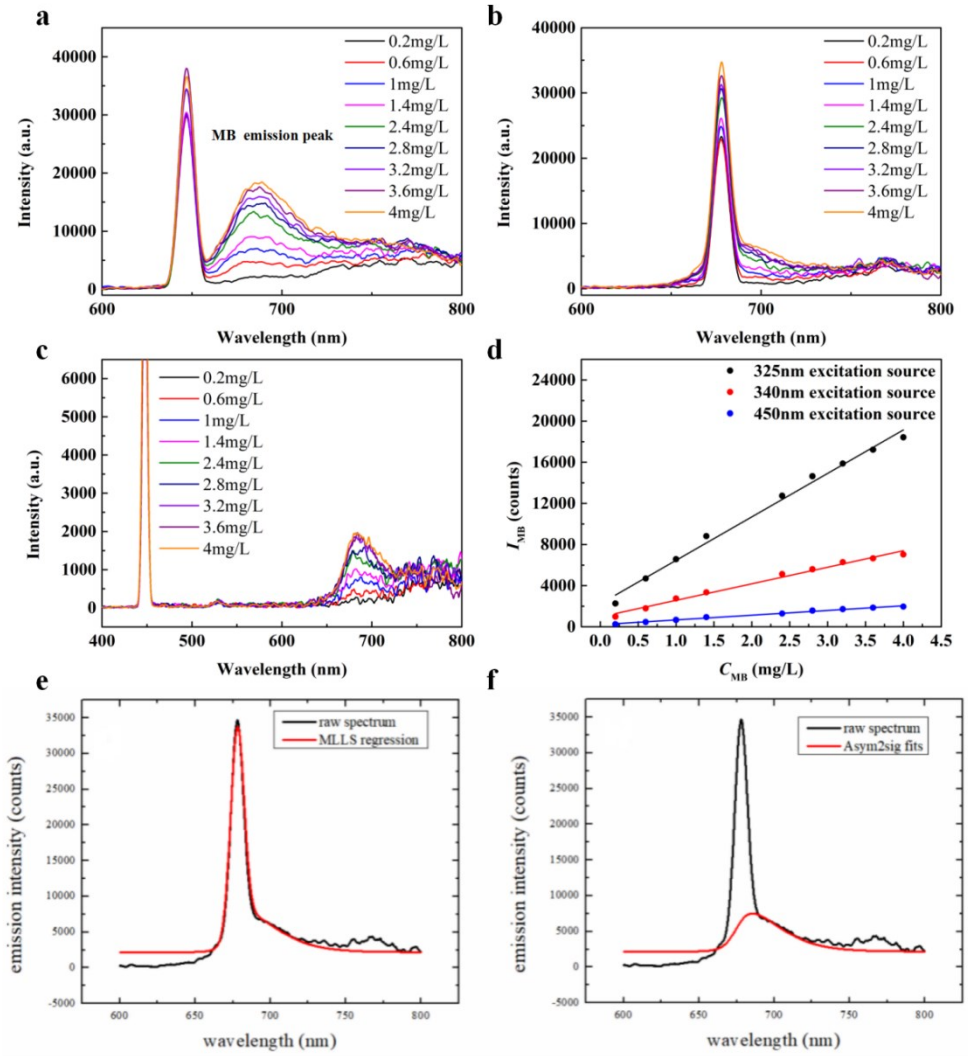

Fig S2. MB emission intensity. **a**, under 325 nm excitation wavelengths. **b**, under 340 nm excitation wavelengths. **c**, under 450 nm excitation wavelengths. **d**, MB concentration $\boldsymbol{C}_{MB}$ as a function of MB emission intensity $\boldsymbol{I}_{MB}$ under 340 nm, 340 nm, and 450 nm excitations. **e,** MLLS regression of overlapped MB emission spectrum. **f,** Asym2sig distribution extracted from MLLS fitting.

Section 3: Construction of time dependent MB fluorescence intensity differential component

As shown in Eq (14), the time dependent MB fluorescence intensity differential component can be used to determine external in-band quantum yield in certain band diagram. In this section, the CZA sample illuminated with 325 nm excitation wavelength is used as an example for determining fluorescence intensity differential component ($\frac{dI_F(t)}{dt}$ in Eq (14)). As exhibited in Eq (12), the accurate determination of $I_{F(t)}$ requires construction of fractional photolysis profile $\alpha_{photolysis}(t)$ and fractional sample scattering profile ($e^{-\mu_s F(t)l}$). For fractional photolysis profile $\alpha_{photolysis}(t)$ measurement, the pure MB were excited with different incident wavelength (Fig. S1(c-j)), only 325 nm excitation could render a proper photolysis. Therefore, the photolysis under 325 nm excitation is studied on MB pure pollutant with different MB concentration. The results are shown in Fig. S3.

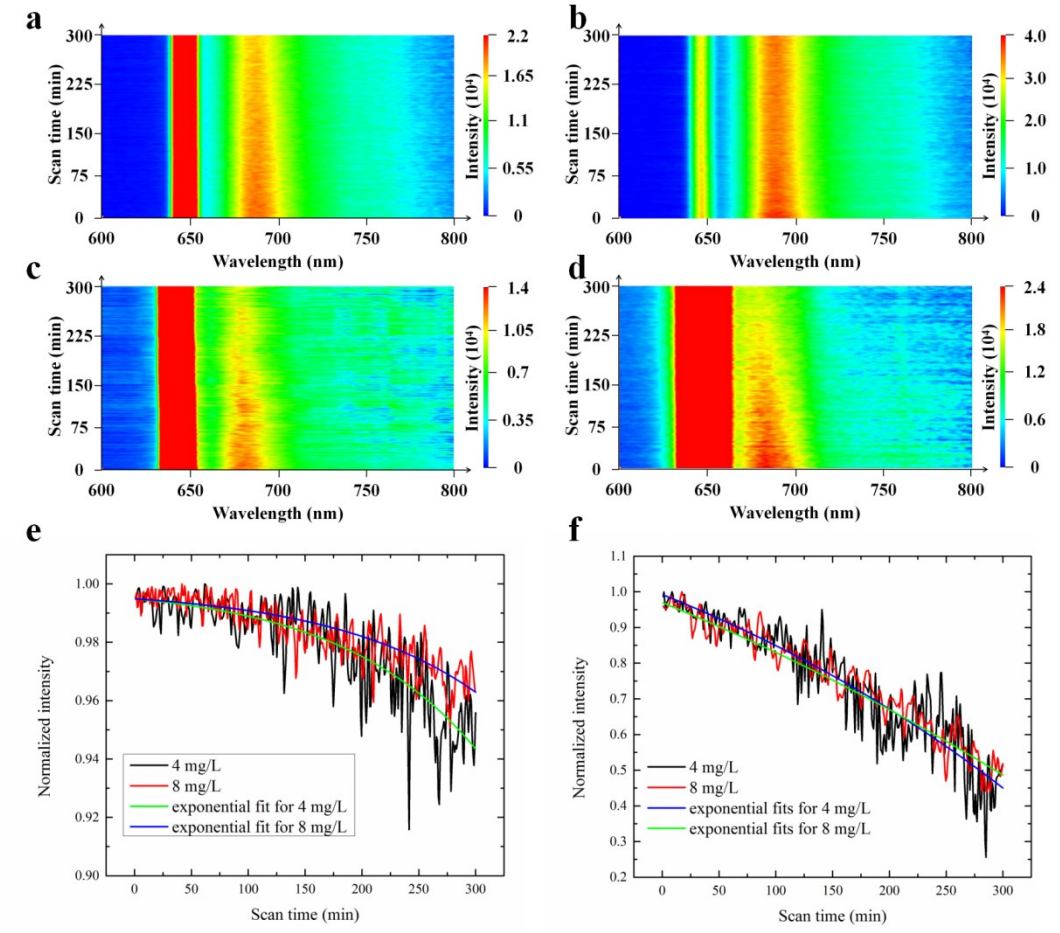

Fig. S3. The rate of degradation MB solution with different MB concentration under 325 excitation wavelength. **a**, 4 mg/L without sample. **b**, 8 mg/L without sample. **c**, 4 mg/L with CZA samples. **d**, 8 mg/Lwith CZA samples . **e**, the comparison between the Fig S4a and S4b. **f**, the comparison between the Fig S4c and S4d.

As in Fig S3a, b and e, the diverse proportion of 8 mg/L and 4 mg/L pure MB degradation was observed under 325 nm ultra-violet illumination. As in Fig S3e, according to equation (8) in manuscripts, after fitting the experimental spectrum with exponential decay function, according to Eq (11) the fractional photolysis profile ($\alpha_{\text{photolysis}}(t)$) can be obtained by dividing the $I_F(t)$ profile with $I_F(0)$. Therefore, the statistics shows the 4 mg/L pure MB can be degraded 5.6% within 300 min acquisition time. By applying the same approach to analyze 8 mg/L pure MB

degradation under 325 nm excitation (Fig S3 b and e), the statistics reveals a 3.4 % pure MB decomposing (MB florescence intensity is decreased from 40683 to 39297). The results in Fig S3c, d and f are used to analyze the photocatalytic activity as a function of pollutant concentration. For different concentrations of MB, the 0.25 g CZA NPs could produce an approximate equal MB degradation profile. Therefore, the MB photolysis rate is correlated with pollutant concentration, while the MB degradation attributed to the photocatalytic activity seems to be weakly influenced by pollutant concentration.

For determining the fractional sample scattering profile ($e^{-\mu_S F(t)l}$), the experiments should be conducted under excitation wavelength longer than 325 nm, where the fractional photolysis profile ($\alpha_{photolysis}(t)$) remains constant during the experiment procedure ($\alpha_{photolysis}(t)=1$). Therefore, the correlation between $I_F(t)$ and $I_{measured}(t)$ in Eq (12) is only relevant with the fractional sample scattering profile ($e^{-\mu_S F(t)l}$).

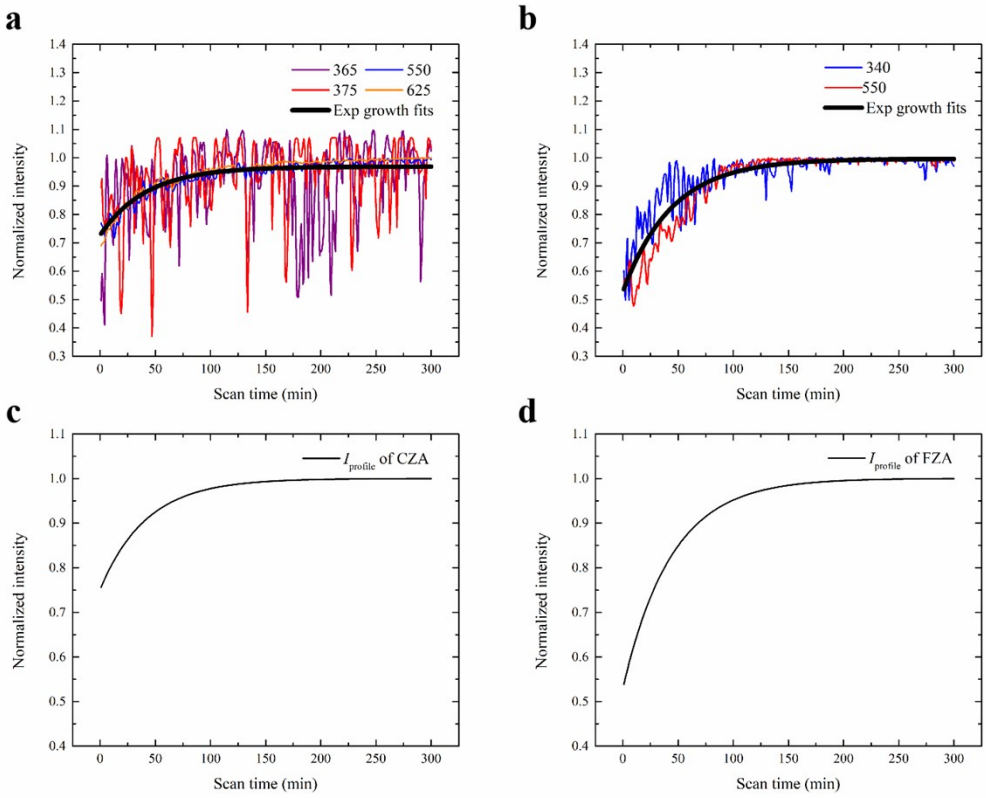

Fig. S4 a, measured $I_{\text{scattering profile}}$ of CZA sample under versus excitation wavelength. **b**, measured $I_{\text{scattering profile}}$ of FZA sample under versus excitation wavelength. **c,** $I_{\text{scattering profile}}$ of CZA modelled by exponential growth function. **d,** $\boldsymbol{I}_{\text{scattering profile}}$ of FZA modelled by exponential growth function.

By dividing the recorded time dependent maximum MB florescence intensity with 4 mg/L MB fluorescence intensity (I_F) at specific excitation wavelength for CZA and FZA samples, their individual fractional sample scattering profile($e^{-\mu sF(t)l}$) in manuscripts equation (9) can be obtained by fitting an exponential growth function to the recorded spectra (Fig. S4). If the fractional sample scattering profile ($e^{-\mu sF(t)l}$) value at the end of experiment saturated to 1, it can prove the validity of the profile construction.

Since the in-situ measured MB florescence profile ($\boldsymbol{I}_{\text{measured}}$ (t) in manuscripts equation (9)) is the superposition of fractional sample scattering profile($e^{-\mu sF(t)l}$) and

fractional photolysis profile ($\alpha_{photolysis}$(t)). The MB real degradation model ($I_F(t)$ in manuscripts equation (10) can be obtained

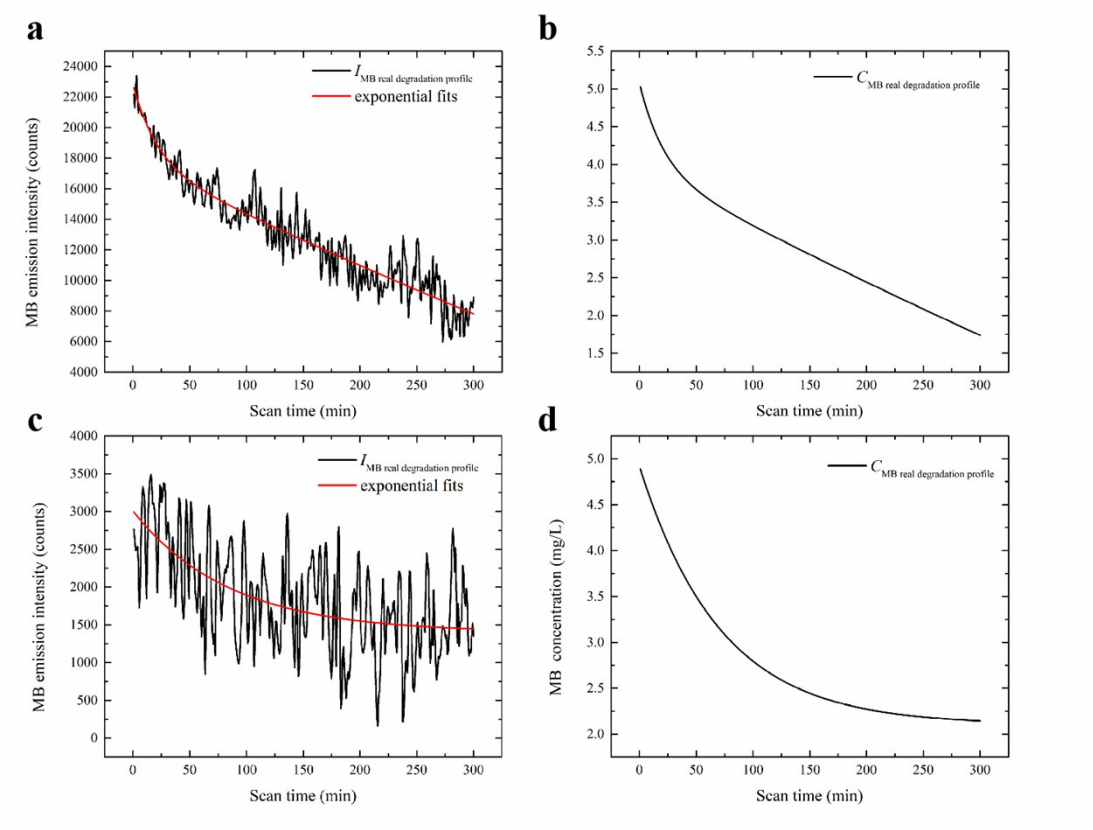

Fig. S5. a, $\boldsymbol{I}_F(t)$ profile under 325 nm excitation. **b**, $\boldsymbol{C}_{MB\ profile}$ under 325 nm excitation. **c**, $\boldsymbol{I}_F(t)$ profile under 450 nm excitation. **d**, $\boldsymbol{C}_{MB\ profile}$ under 450 nm excitation.

By taking the $I_{measured}$ (t) profile for CZA sample excited with 325 nm and 450 nm wavelength, After excluding the photon-particle scattering effect and pure MB photolysis, the time dependent MB fluorescence profile under 325 nm and 450 nm are exhibited in Fig. S5a, c. After fitting the profile in Fig. S5a,c and differentiating the I_F(t) profile with t, the $\frac{dI_F(t)}{dt}$ profile in Eq (14) can be then obtained. The results are shown in Fig S6. As depicted in Fig. 6, before 50 min photocatalytic process, the MB degradation rate is faster than photocatalytic process after 50 min. This represent the photon scattering events could systematically enhance the EIQY for photocatalytic

activity.

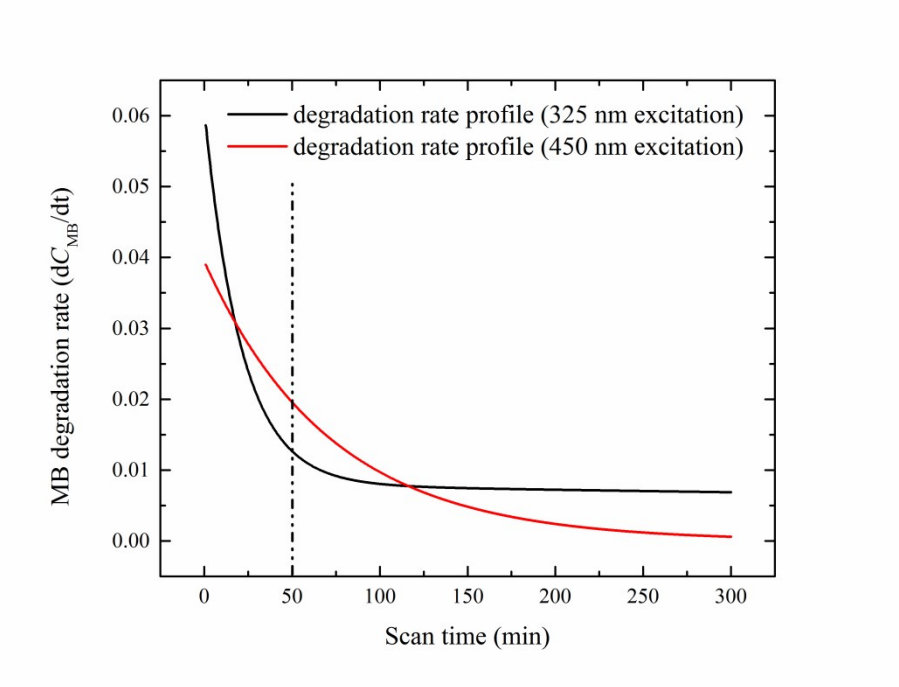

Fig. S6 MB degradation rate as a function of acquisition time.

Section 4: Sample structural characterization

Fig. S7a shows the fabricated CZ nanocomposites. According to JCPD data (04-004-5685), The CuO diffraction peaks were observed in Fig. 7a, which evidences the CuO/ZnO heterostructure formation. The direct evidence of CuO deposition on ZnO surface is presented by the TEM image in Fig. S7b. The investigated CZA sample was confirmed to have CuO/ZnO/Ag double heterostructures in our recent report [1], the evidence of ZnO/Ag heterojunction formation in ZA sample can be found and the structural details of FZA sample is described in our recent publications [2,3].

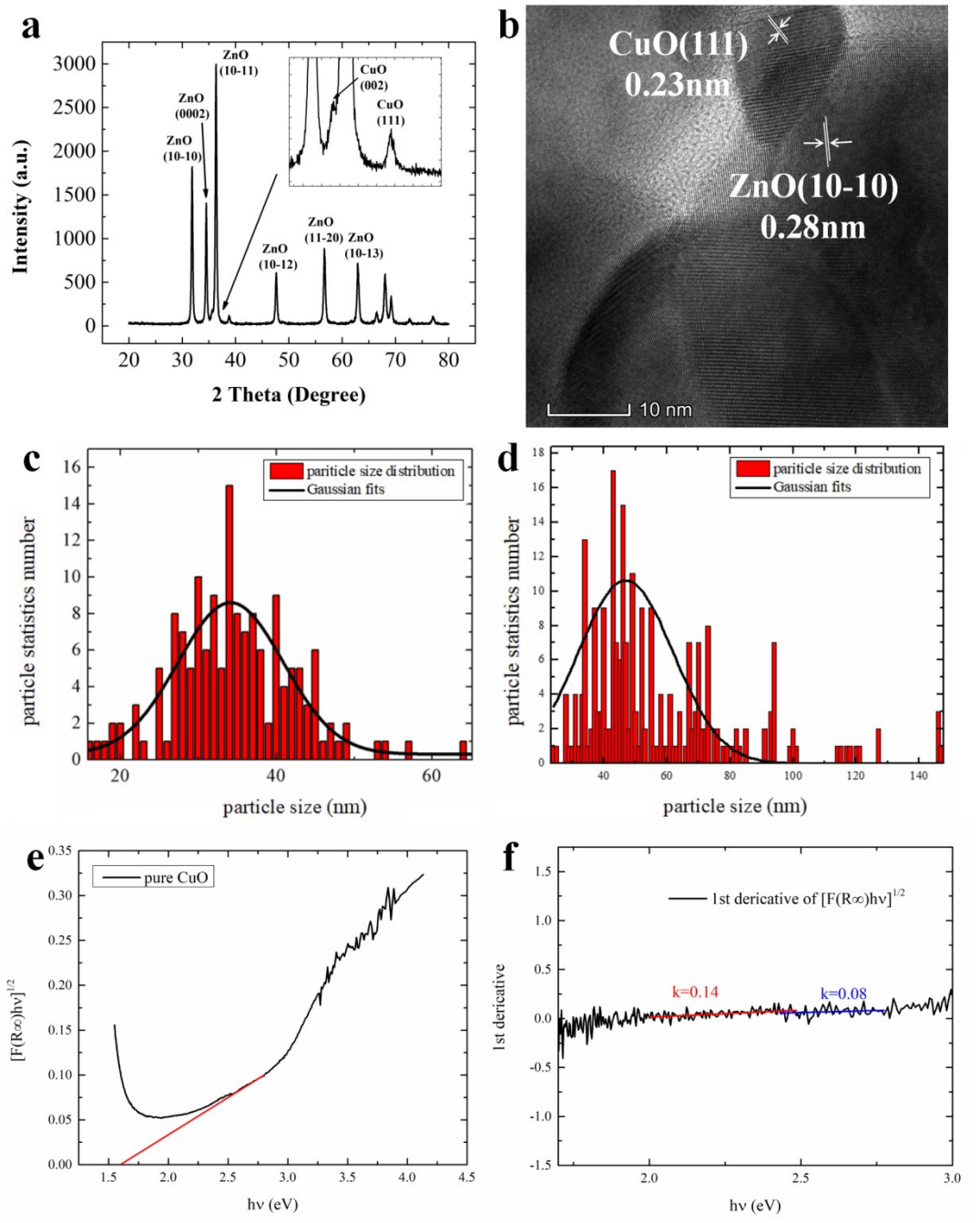

Fig. S7. Structure properties of samples. a, XRD spectrum of the CZ sample. **b**, HRTEM image of the ZnO/CuO heterostructure. **c**, histogram of FZA particle size distribution. **d**, histogram of CZA particle size distribution. **e**, the band gap of pure CuO calculated by Kubelka-Munk formula of UV-vis diffuse reflectance spectrum. **f**, the 1st dericative of Fig. S7e.

From SEM images and low magnification images of TEM from our previous study [1,3], the histograms of particle distribution for both samples are shown in Fig. S7c,d.

The nanoparticle size for CZA sample is determined as 46.9 nm±15.2 nm, while the FZA particle size 34.2 nm±6.8 nm.

The UV-vis diffuse reflectance spectra (the range of 300 to 800 nm) in Fig. S7e,f were obtained using a Perkin Elmer Lambda 650 spectrophotometer with an integral sphere. By applying the Kubelka-Munk formula (K-M) to the recorded spectrum, and selecting the range for the smallest slope in first derivative spectrum, the band gap CuO for CZA was extrapolated as 1.6 eV, which further support the validity of constructed band diagram.

References

1. M. Xu, Y. Chen, W.Y. Hu, et al. Designed synthesis of microstructure and defect-controlled Cu-doped ZnO–Ag nanoparticles: exploring high-efficiency sunlight-driven photocatalysts. *J. Phys. D: Appl. Phys.* 2019, 53(2): 025106.

2. Y.T. Liu, et al. Novel and efficient synthesis of Ag-ZnO nanoparticles for the sunlight-induced photocatalytic degradation. *Appl. Surf. Sci.* 2019, 476: 632-640

3. J. Zhang, K. Luo, K. Zhao, et al. A synergistic boost of photo-activity of ZnO for photocatalytic degradation of methylene blue by Ag decoration and Fe doping. *Mater. Lett*. 2021, 286: 129250.